https://doi.org/10.17221/102/2025-CJAS

The impact of folic acid on genome-wide DNA methylation profiles in the liver of broilers

Yuting Pang, Yujie Zhang, Yunheng Liu, Xiuling Li, Jinyi Xing**

School of Life Sciences, Linyi University, Linyi, P.R. China

**Corresponding authors: lixiuling@lyu.edu.cn; xingjinyi@lyu.edu.cn*

Citation: Pang Y.T., Zhang Y.J., Liu Y.H., Li X.L., Xing J.Y. (2026): The impact of folic acid on genome-wide DNA methylation profiles in the liver of broilers. Czech J. Anim. Sci., 71: 330–341.

Abstract: Folic acid (FA) plays an important role as a cofactor and coenzyme in animal growth and development, and in the regulation of gene expression and methylation. However, the epigenetic mechanism by which dietary FA supplementation regulates lipid metabolism in broilers remains largely unknown. Therefore, this study aimed to investigate the effects of FA on genome-wide DNA methylation profiles in broiler liver and to identify differentially methylated genes (DMGs) and pathways associated with lipid metabolism. Reduced representation bisulphite sequencing (RRBS) was performed to analyse genome-wide DNA methylation profiles in liver tissues of broilers supplemented with 0 (control, C group), 5 (M group) or 10 mg/kg (H group) FA in basal diet for 42 days. The genome-wide methylation analysis showed that the average percentage of each sample of CpG (5'-C-phosphate-G-3') methylation efficiency was 29.47%. A total of 1 402 differentially methylated regions (DMRs) were detected between C and M groups, including 745 hyper-DMRs and 657 hypo-DMRs, Compared with the C group, 410 hyper-DMRs and 436 hypo-DMRs were identified in the H group. Additionally, 511 hyper-DMRs and 560 hypo-DMRs were found between the M and H group. Furthermore, a total of 134 DMGs exhibited DMRs in the promoter region across all three comparison groups, including 27 upregulated DMGs and 20 downregulated DMGs. Gene Ontology (GO) analysis of DMRs revealed that the associated genes are mainly involved in H3-K4 demethylation, histone lysine demethylation, peptidyl-lysine methylation, histone demethylation, lysine *N*-methyltransferase activity, fat cell proliferation, cellular lipid metabolic processes, fatty-acyl-CoA binding. In addition, key Kyoto Encyclopaedia of Genes and Genomes (KEGG) pathways were primarily associated with the Toll-like receptor signalling pathway, fatty acid metabolism, butanoate metabolism, retinol metabolism. Taken together, these results demonstrated that FA supplementation affects genome-wide DNA methylation profiles in the liver of broilers, suggesting an underlying epigenetic mechanism for its regulation of hepatic lipid metabolism.

Keywords: broilers; DNA methylation; folic acid; lipid metabolism; liver

At present, the fat deposition (especially that of abdominal fat) in broiler chickens is increasing, which seriously affects the quality of chicken meat, reduces feed conversion efficiency and increases the incidence of broiler-specific diseases (Liu et al. 2022; Du et al. 2023). Therefore, reducing the accumulation of abdominal fat in chickens is a major challenge the poultry sector is facing (Liu et al.

Supported by the Nature Science Foundation of Shandong Province of China (Grant No. ZR2017LC018).

https://doi.org/10.17221/102/2025-CJAS

2024). In addition to genetic and environmental factors, nutrition regulation is an effective means of reducing the chicken fat deposition.

Folic acid (FA) is a water-soluble vitamin, belonging to vitamin B9. It is one of the essential micronutrients for animal growth. As a methyl donor, FA can directly be involved in the synthesis and maintenance of RNA, DNA, and protein, as well as DNA in methylation and epigenetic modification (Friso et al. 2017). FA is taken up from the small intestine and then it enters the liver through the portal vein. As one of the major metabolic organs, the liver is a major site of storage and metabolism of FA and is also responsible for methylation reactions (Ma et al. 2025), as recent studies have shown that the folate status critically influences hepatic lipid homeostasis (Chi et al. 2024).

DNA methylation is one of the earliest epigenetic changes that has been discovered to exist in all higher organisms. It is closely related to biological processes such as gene silencing, inactivation of the X chromosome, genomic imprinting, RNA interference and the silencing of repeat DNA elements (Angeloni and Bogdanovic 2019; Mattei et al. 2022). In general, DNA methylation acts as a suppressor of gene expression (Mattei et al. 2022).

Several studies have explored the effects of folic acid on gene expression and DNA methylation. FA has been reported to increase methylation of the C/EBPα gene promoter and to reduce the expression of this gene in preadipocytes in chickens (Yu et al. 2014). In broilers, an *in ovo* injection of 150 μg FA on embryonic day 11 upregulated *IGF2* expression by modulating DNA hypomethylation and improving chromatin accessibility in the gene promoter region (Liu et al. 2016). Similarly, a previous study showed that dietary FA supplementation significantly increased serum IGF2 concentrations and *IGF2* mRNA expression in abdominal fat, but the methylation of the *IGF2* promoter was not affected by FA addition (Li et al. 2021). Furthermore, FA enhanced differentiation and mRNA expression of myogenin and influenced genome-wide DNA methylation levels in C2C12 cell lines (Li et al. 2018). Recent evidence from mammalian models further underscores the role of FA in hepatic lipid regulation. Yang et al. (2025) comprehensively reviewed that folate regulates hepatic lipid metabolism through one-carbon metabolism and DNA methylation, affecting pathways such as methionine metabolism and lipid signalling. Chi et al. (2024) reported that disturbed folate-mediated one-carbon metabolism impairs autophagic flux and increases hepatocytic lipid accumulation. Wen et al. (2025) further demonstrated that folic acid promotes autophagy to relieve the metabolism-associated fatty liver disease by regulating NRF2. In poultry, Sun et al. (2024) showed that dietary FA supplementation alleviates the fatty liver syndrome in laying hens by modulating lipid metabolism-related gene expression. However, how FA influences chicken liver fat metabolism through epigenetic mechanisms remains unclear.

To date, the impact of FA on broiler DNA methylation has remained understudied. The objective of this study was to investigate DNA methylation patterns in the liver of broilers supplemented with normal, medium, or high levels of FA (0, 5 and 10 mg/kg, respectively) in the basal diet. Reduced representation bisulphite sequencing (RRBS) was performed to systematically identify differentially methylated regions (DMRs) and differentially methylated genes (DMGs) associated with FA supplementation and hepatic fat metabolism. Our findings will provide evidence that FA may influence liver lipid metabolism through alterations in DNA methylation profiles.

MATERIAL AND METHODS

Experimental procedures and diets. The animal procedures were reviewed and approved by the Animal Care Committee of Linyi University.

A total of 270, 1-day-old female broilers with an average body weight of 46 ± 0.9 g were randomly allotted to three dietary treatments supplemented with 0 mg/kg (control group, marked as C), 5 mg/kg (marked as M), 10 mg/kg (marked as H) folic acid (FA) in basal diet for 42 days. Each treatment had six replicate cages with 15 birds per cage. The dosages of 5 and 10 mg/kg FA were selected based on the NRC (1994) requirement for broilers (0.55 mg/kg) and on our previous studies demonstrating that these dosages effectively modulate growth performance, fat deposition, and gene expression in the same experimental model (Li et al. 2021; Zhang et al. 2021). A standard basal diet containing maize and soybean meal [composition shown in Electronic Supplementary Material (ESM) Table S1] was fed as mash. The basal diet was formulated to meet or exceed the nutritional

https://doi.org/10.17221/102/2025-CJAS

requirements for broiler chickens at the Feeding Standard of Chickens (NY/T33-2004; P.R. China). Water and mash feed were provided *ad libitum*, with conventional vaccination and natural lighting during the experimental period.

Sampling, DNA and RNA extraction. At 42 days of age, one bird of approximately average weight was randomly selected from each replicate group, fasted for 12 h and then euthanised. After slaughter, some of the liver samples were immediately isolated, washed briefly with PBS, frozen in liquid nitrogen and stored at –80 °C for total extraction of DNA and RNA. Genomic DNA was isolated from fresh-frozen liver tissue using the Genomic DNA Purification Kit (Thermo Fisher Scientific, Shanghai, P.R. China) according to the manufacturer's protocols. Then genomic DNA was quantified using a NanoDrop spectrophotometer and Qubit Fluorometer.

Total RNA was isolated from liver samples (the same samples as above) by using Trizol Reagent (Invitrogen, Carlsbad, USA) according to the manufacturer's instructions, and it was quantified spectrophotometrically.

Reduced representation bisulphite sequencing (RRBS). The construction of the DNA methylation library was performed at BioGenius (Shanghai, China) using reduced representation bisulphite sequencing (RRBS). The RRBS library was constructed using 2 μg of high-quality genomic DNA, and for each group, an equal amount of DNA from six samples was combined to create three DNA pools, respectively. Briefly, genomic DNA was digested with the restriction enzyme *Msp*I to enrich the CpG region. The resulting DNA fragments were end-repaired and the base "A" was added to the 3' ends, to enable ligation with sequencing adapters containing a complementary "T" overhang. DNA fragments of appropriate size (250–500 bp) were selected by electrophoresis and purified, and the recovered fragments were treated with bisulphite. After desalting, DNA fragments with connectors at both ends were amplified by PCR to construct the sequencing library. Finally, the quality of each constructed library was tested, and qualified libraries were used for cluster preparation and sequencing by Illumina HiSeq X Ten (Illumina Inc., San Diego, CA, USA).

RRBS data analysis. First, raw sequencing reads were filtered to obtain clean reads. The filtered high-quality sequencing data were compared with the chicken reference genome (*Gallus_gallus*-5.0) using Bismark (v0.7.4) with default parameters for paired-end reads. Methylation calls were subsequently extracted from the alignment results. The length of the compared seed region was set to 50 bases, and one mismatch was allowed within the seed region. After alignment, PCR duplicates were removed, and the methylation status at each cytosine was determined by calculating the weighted methylation level. Subsequently, the statistics of genome comparison results, the coverage of sequencing data in CpG island and promoter region, the respective proportions of CG, CHG, and CHH methylation types, and the distribution of methylation sites in CpG island and promoter regions were calculated. Finally, differentially methylated regions (DMRs) were identified using the MethylKit R package. According to the distribution of DMRs in the whole genome, DMRs associated genes were defined. The nearest neighbour genes of differentially methylated regions were annotated (Gene Ontology, GO) by the GOseq R package. The differentially methylated genes (DMGs) were analysed by the KEGG pathway to determine the significantly enriched GO entries and signal pathways by correcting $P < 0.05$.

Integration with transcriptome data. Our RRBS data were integrated with previously published liver transcriptome data from the same experimental model (Zhang et al. 2021) to examine the overlap between DMGs and DEGs, particularly for genes involved in lipid metabolism.

Validation of RRBS data using bisulphite sequencing PCR (BSP). RRBS results were validated by bisulphite sequencing PCR (BSP). Methylation primers were designed using the MethPrimer sofware (http://www.urogene.org/methprimer/) (ESM Table S2). The sodium bisulphite treatment of chicken genomic DNA (extracted from the same sample used for RRBS) was performed using the EZ DNA Methylation-Gold Kit (Zymo Research, CA USA). PCR amplification was carried out with Ex Taq® Hot Start Version (TaKaRa, Beijing, P.R. China). PCR products were gel purified and cloned into the pMD18-T vector (TaKaRa, Beijing, P.R. China). For each sample, 10~13 positive clones were selected and sequenced. All the sequences were analysed using BiQ Analyser v2.0.

Reverse transcription-quantitative real-time PCR (qRT-PCR). First-strand cDNA was synthesized from 2 μg total RNA using a reverse transcrip-

https://doi.org/10.17221/102/2025-CJAS

tion kit (Promega, Madison, USA) according to the manufacturer's instructions. The primer sequences used for these reactions are listed in ESM Table S2. Quantitative real-time PCR (qRT-PCR) was carried out with the Brilliant SYBR Green qRT-PCR Master Mix (Stratagene, La Jolla, CA, USA). All PCR reactions were performed in triplicate with negative controls. Using the *ACTB* gene for normalization, the relative expression levels of *ECE1* and *METTL21A* were analysed by the $2^{-\Delta\Delta CT}$ method.

Statistical analysis. Data were analysed by one-way ANOVA, followed by Tukey's honestly significant difference (HSD) test using SAS v9.4 software (SAS Institute Inc., Cary, NC, USA). All experiments were performed with three biological replicates per group (n = 3), and each biological replicate consisted of pooled samples from three individual broilers. The GO and KEGG analyses were performed using Fisher's exact test. Graphs were generated using GraphPad Prism v8.0 (GraphPad Software, San Diego, CA, USA). The level of significance was set at $P < 0.05$.

RESULTS

Data quality evaluation. The sequencing data quality was rigorously evaluated to ensure the reliability of subsequent methylation analyses. As shown in Figure 1, the sequencing quality was high, with the Q20 score reaching 95%, indicating that the raw data were suitable for further analysis. Furthermore, the bisulphite conversion rate, assessed using unmethylated lambda DNA as a control, was 95.5%. This high conversion efficiency (>95%) confirms the effectiveness of the bisulphite treatment and minimises the risk of false-positive methylation calls, thereby validating the accuracy of the identified DNA methylation profiles.

Reference genome alignment. Using Bismark, the downstream data were aligned with the *G. gallus* reference genome. The seed length for alignment was set to 50 bp, and each read was allowed to have one mismatch within the seed region. The alignment efficiency for each sample is listed in Table 1. Filtered read pairs were uniquely aligned to the reference sequence with unique mapping efficiencies of 19.90%, 19.00% and 18.20% for C, M and H groups, respectively (Table 1). The genome-wide methylation analysis indicated that the average percentage of CpG methylation efficiency

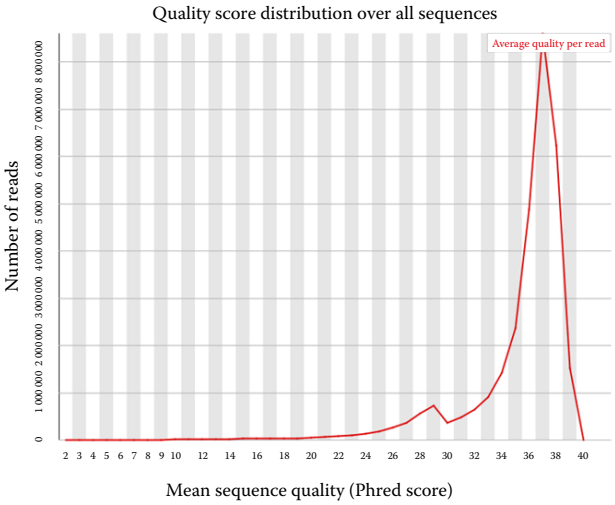

Figure 1. Base quality distribution
The horizontal coordinate indicates the base mass value, and the vertical coordinate indicates the number of reads whose base mass average is a specific value

per sample was 29.47%. However, the percentage of methylation in CHG and CHH contexts was only 0.20% and 0.3%, respectively. It can be seen that the DNA methylation level of chicken liver tissue detected in this experiment mainly occurred at CpG sites, and the DNA methylation levels in both CHH and CHG contexts were low, which did not contribute very much to the overall methylation level and therefore no further studies were performed.

Methylation of bases. Methylation of single base pairs was detected (methylation calling with low-quality bases <20 was filtered out). For paired reads that passed the quality control, the 5' end sequencing results were used. The methylation status of each C base was determined in each sample. CpG coverage and methylation levels for three groups are presented in Figures 2 and 3. The results indicate that the generated libraries contained a considerable number of reads with high coverage (>10×) of the CpGs. Moreover, a single peak on the left-hand side of the histogram was observed for three groups (Figure 2). The CpG coverage was essentially the same across all groups, indicating that the data were highly reliable. Figure 3 shows that the CpG methylation levels in all three groups exhibit a bimodal distribution, mainly distributed in the fully methylated (100%) or fully unmethylated (0%) areas. However, there was not much difference in unmethylated or fully methylated areas between the three groups.

https://doi.org/10.17221/102/2025-CJAS

Table 1. The alignment efficiency of each sample

Statistics	Sample ID	C	M	H
Basic data production	raw reads pairs	29 883 922	33 979 485	31 004 817
	raw data amount (bp)	8 965 176 600	10 193 845 500	9 301 445 100
	filtered reads pairs	27 455 824	31 301 734	28 698 296
	alignments (pairs)	5 477 414	5 940 858	5 214 885
	mapping efficiency	19.90%	19.00%	18.20%
	no alignments (pairs)	21 606 022	24 951 695	23 135 544
	pairs did not map uniquely	372 388	409 181	347 867
Final cytosine methylation report	total number of C's analysed	392 597 328	425 077 019	363 249 838
	total methylated C's in CpG context	19 897 020	22 633 772	17 827 967
	total methylated C's in CHG context	260 933	278 177	225 041
	total methylated C's in CHH context	604 775	667 432	599 744
	total unmethylated C's in CpG context	47 285 209	54 290 328	42 813 030
	total unmethylated C's in CHG context	106 240 177	116 557 070	98 967 361
	total unmethylated C's in CHH context	218 309 214	230 650 240	202 816 695
	C methylated in CpG context	29.60%	29.40%	29.40%
	C methylated in CHG context	0.20%	0.20%	0.20%
	C methylated in CHH context	0.30%	0.30%	0.30%

bp = base pair(s); C = control group (0 mg/kg FA); CHG = non-CpG methylation sequence context; CHH = non-CpG methylation sequence context; CpG = cytosine-phosphate-guanine dinucleotide; H = high folic acid group (10 mg/kg FA); M = medium folic acid group (5 mg/kg FA)

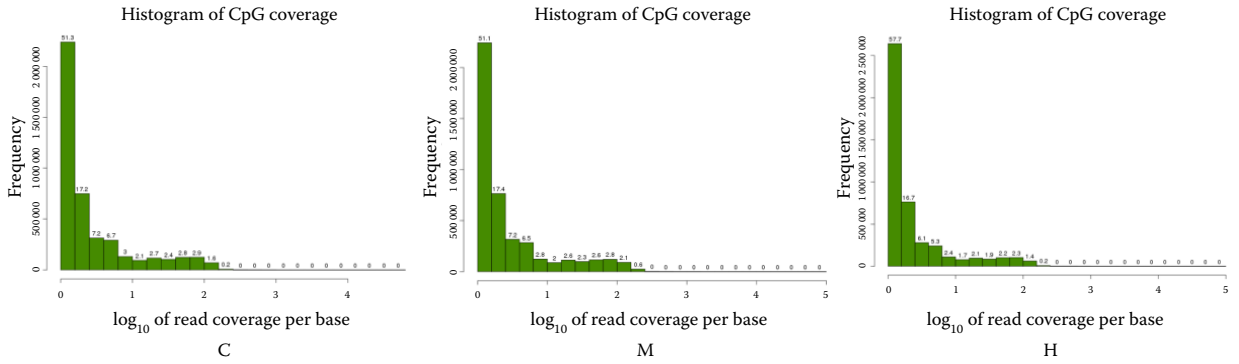

Figure 2. The histogram of CpG coverage

The x-axis indicates $\log_{10}$ values corresponding to the number of reads per CpG and y-axis represents the number of reads C = control group (0 mg/kg FA); CpG = cytosine-phosphate-guanine dinucleotide; M = medium folic acid group (5 mg/kg FA); H = high folic acid group (10 mg/kg FA)

Identification of differentially methylated regions (DMRs). Three comparative combinations were selected for DMR identification, and the number of hyper and hypo-DMRs is listed in Table 2. There were 745 hyper-DMRs and 657 hypo-DMRs between C and M groups. The H group had 410 hyper-DMRs and 436 hypo-DMRs compared to the C group. A total of 1 071 DMRs were detected between the M and H groups, including 511 hyper-DMRs and 560 hypo-DMRs. The top 10 significant DMRs for each comparison group are shown in ESM Table S3.

Distribution of DMRs in different functional regions of genes. In order to further analyse the methylation changes at CpG sites, this study annotated the DMRs among different groups according to the functional regions of genes. The results revealed that most of the DMRs were located in intergenic

https://doi.org/10.17221/102/2025-CJAS

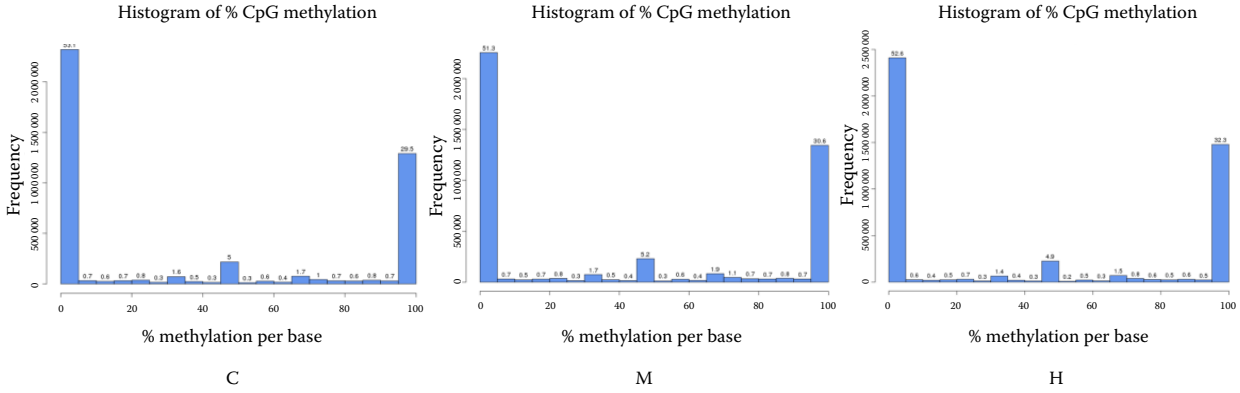

Figure 3. The histogram of % CpG methylation

The x-axis indicates percent methylation at each cytosine site and y-axis denotes the number of CpGs

C = control group (0 mg/kg FA); CpG = cytosine-phosphate-guanine dinucleotide; M = medium folic acid group (5 mg/kg FA); H = high folic acid group (10 mg/kg FA)

Table 2. The number of hyper and hypo-DMRs in each comparison group

Samples	All DMRs	Hyper-DMRs	Hypo-DMRs
C vs M	1 402	745	657
C vs H	846	410	436
M vs H	1 071	511	560

C = control group (0 mg/kg FA); DMR = differentially methylated region; H = high folic acid group (10 mg/kg FA); M = medium folic acid group (5 mg/kg FA)

regions (78–80%), about 3–5% in exons, 11–13% in introns, and 4–5% in promoter regions (Figure 4). DMRs for each comparison group (C, M and H) were categorised as reoccurring either in CpG islands, shores, or other regions. Among all CpG sites showing methylation differences, 19–22% were located in CGI, and 27–30% were in CpG shores (Figure 5). No significant differences in DMRs were observed between the comparison groups.

Detection of differentially methylated genes (DMGs) in promoter region. The DMGs between two groups were identified based on associated genes. By comparing the DMRs detected in the three comparison groups with the chicken reference genome, 541, 496, and 480 genes were found to be covered, respectively (Table 3). A total of 134 DMGs exhibited DMRs in the promoter region across all three comparison groups, including 27 upregulated DMGs and 20 downregulated DMGs (Figure 6). The top 10 significant DMGs in each comparison group are shown in ESM Table S4.

GO enrichment analysis. The general gene classifications based on the significant GO terms of biological processes (BP), cellular components (CC) and molecular functions (MF) are shown in Table 4. The GO enrichment analysis results demonstrated that there were 401 (BP), 45 (CC), and 102 (MF) significantly enriched GO terms in the three comparison

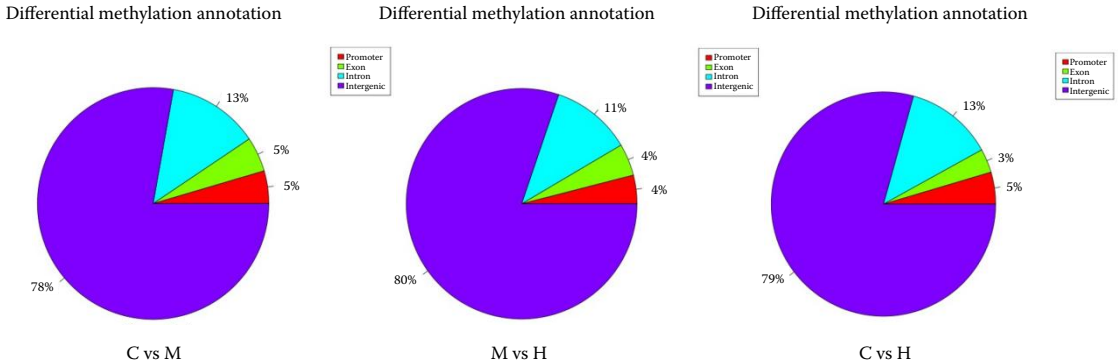

Figure 4. Percentages of gene structure categories of differential sites within the intergenic area

C = control group (0 mg/kg FA); H = high folic acid group (10 mg/kg FA); M = medium folic acid group (5 mg/kg FA)

https://doi.org/10.17221/102/2025-CJAS

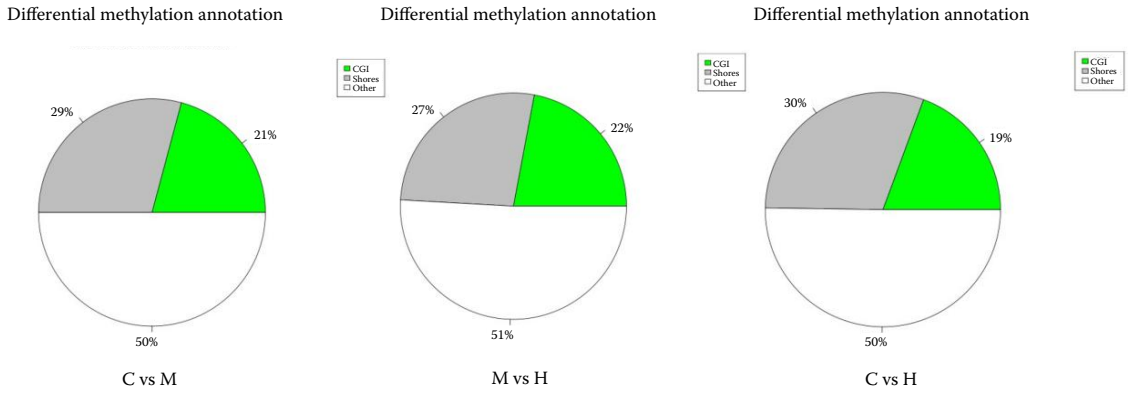

Figure 5. Percentages of CpG categories (islands, shores, or other) for significant differential DNA methylation loci
C = control group (0 mg/kg FA); CGI = CpG island; H = high folic acid group (10 mg/kg FA); M = medium folic acid group (5 mg/kg FA); shores = CpG island shores

Table 3. The number of DMGs in the promoter region

Groups	All DMGs	Up-regulated DMGs	Down-regulated DMGs
C vs M	541	274	267
C vs H	496	256	240
M vs H	480	268	212

C = control group (0 mg/kg FA); DMG = differentially methylated gene; H = high folic acid group (10 mg/kg FA); M = medium folic acid group (5 mg/kg FA)

groups, respectively. Many of the top enriched GO terms had important regulatory functions, such as H3-K4 demethylation (GO: 0034720), histone lysine demethylation (GO: 0070076), peptidyl-lysine methylation (GO: 0018022), histone demethylation (GO: 0016577), lysine *N*-methyltransferase activity (GO: 0016278), fat cell proliferation (GO: 0070341), cellular lipid metabolic process (GO: 0044255), fatty-acyl-CoA binding (GO: 0000062), etc. Notably, fat metabolism and methylation genes were also significantly enriched, including *AACS*, *FABP5*, *IRF-4*, *EPHX2*, suggesting folic acid may regulate the expression of these genes in broilers. The top 10 significantly enriched GO terms in each comparison group are listed in ESM Table S5.

KEGG pathway analysis. KEGG pathway analysis was performed to investigate the functions of DMGs in response to folic acid. The significantly enriched pathways are listed in Table 5. In the comparison between the C and M groups, 16 pathways showed significant enrichment, including butanoate metabolism, fatty acid degradation, tryptophan metabolism, biosynthesis of antibiotics, among others, involving 83 genes. For C group vs H group, only four significant pathways were identified, including the Toll-like receptor signalling pathway, influenza A, salmonella infection, and

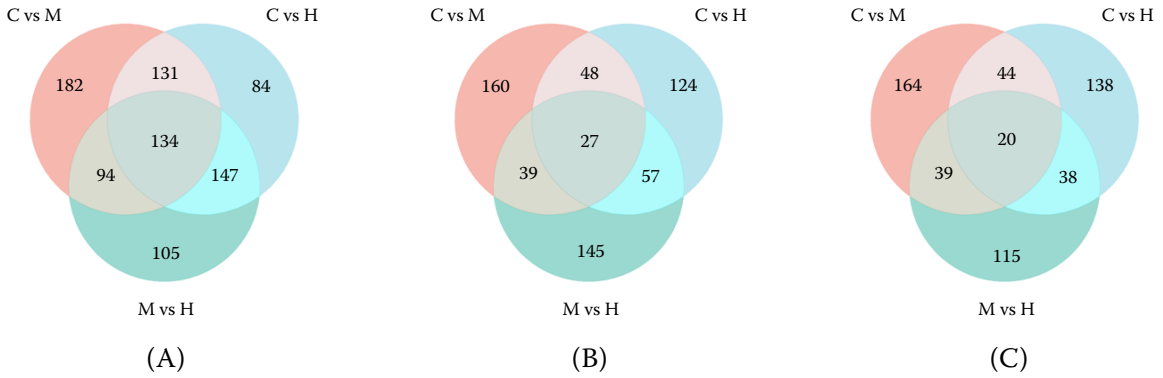

Figure 6. Venn diagram of DMGs in all three comparison groups
(A) All DMGs; (B) Up-regulated DMGs; (C) Down-regulated DMGs
C = control group (0 mg/kg FA); DMG = differentially methylated gene; H = high folic acid group (10 mg/kg FA); M = medium folic acid group (5 mg/kg FA)

https://doi.org/10.17221/102/2025-CJAS

Table 4. GO terms enriched of DMGs in each comparison group

Groups	BP		CC		MF	
	total GO terms	significant GO terms	total GO terms	significant GO terms	total GO terms	significant GO terms
C vs M	3 726	177	406	14	701	49
C vs H	3 385	98	390	11	646	25
M vs H	3 567	126	402	20	690	28

BP = biological process; C = control group (0 mg/kg FA); CC = cellular component; DMG = differentially methylated gene; GO = Gene Ontology; H = high folic acid group (10 mg/kg FA); M = medium folic acid group (5 mg/kg FA); MF = molecular function

Table 5. Significant pathways of DMGs in each comparison group

Groups	Pathway ID	Description	*P*-value	Genes
C vs M	path:gga00650	butanoate metabolism	0.001	5
	path:gga00040	pentose and glucuronate interconversions	0.003	4
	path:gga00071	fatty acid degradation	0.003	5
	path:gga00380	tryptophan metabolism	0.007	5
	path:gga05164	influenza A	0.007	10
	path:gga00280	valine, leucine and isoleucine degradation	0.011	5
	path:gga04672	intestinal immune network for iga production	0.016	4
	path:gga01130	biosynthesis of antibiotics	0.027	11
	path:gga05168	herpes simplex infection	0.033	9
	path:gga00062	fatty acid elongation	0.033	3
	path:gga00130	ubiquinone and other terpenoid-quinone biosynthesis	0.037	2
	path:gga04270	vascular smooth muscle contraction	0.037	7
	path:gga03440	homologous recombination	0.041	3
	path:gga00640	propanoate metabolism	0.041	3
	path:gga00860	porphyrin and chlorophyll metabolism	0.046	3
	path:gga01212	fatty acid metabolism	0.047	4
C vs H	path:gga04620	toll-like receptor signalling pathway	0.021	6
	path:gga05164	influenza A	0.007	9
	path:gga05132	salmonella infection	0.029	5
	path:gga00830	retinol metabolism	0.047	3
M vs H	path:gga00830	retinol metabolism	0.012	4
	path:gga04068	foxo signalling pathway	0.024	8
	path:gga04810	regulation of actin cytoskeleton	0.014	11
	path:gga00071	fatty acid degradation	0.015	4
	path:gga01212	fatty acid metabolism	0.039	4
	path:gga04340	hedgehog signalling pathway	0.042	4
	path:gga04145	phagosome	0.012	9
	path:gga00280	valine, leucine and isoleucine degradation	0.039	4
	path:gga00380	tryptophan metabolism	0.026	4
	path:gga00072	synthesis and degradation of ketone bodies	0.033	2
	path:gga00650	butanoate metabolism	0.032	3

C = control group (0 mg/kg FA); DMG = differentially methylated gene; H = high folic acid group (10 mg/kg FA); M = medium folic acid group (5 mg/kg FA); P = probability; pathway ID = pathway identifier

https://doi.org/10.17221/102/2025-CJAS

retinol metabolism, involving 23 genes. Between M group vs H group, 11 significant pathways were enriched such as retinol metabolism, FoxO signalling pathway, regulation of the actin cytoskeleton, fatty acid metabolism, involving 57 genes with differential methylation.

Integrated analysis of DNA methylation and transcriptome data. Among the 134 DMGs with promoter DMRs identified in this study, 25 genes showed differential expression in the transcriptome data, including key lipid metabolism-related genes such as *ACADL*, *FABP3*, and *HMGCR*. This concordance suggests that FA may regulate the expression of these genes through epigenetic modifications.

RRBS data validation of *ECE1* and *METTL21A* via qRT-PCR and BSP. Candidate genes were identified based on promoter differentially methylated regions (DMRs) identified by RRBS, functional enrichment in lipid metabolism and epigenetic regulation, and correlation between DNA methylation and gene expression. Among these, *ECE1* and

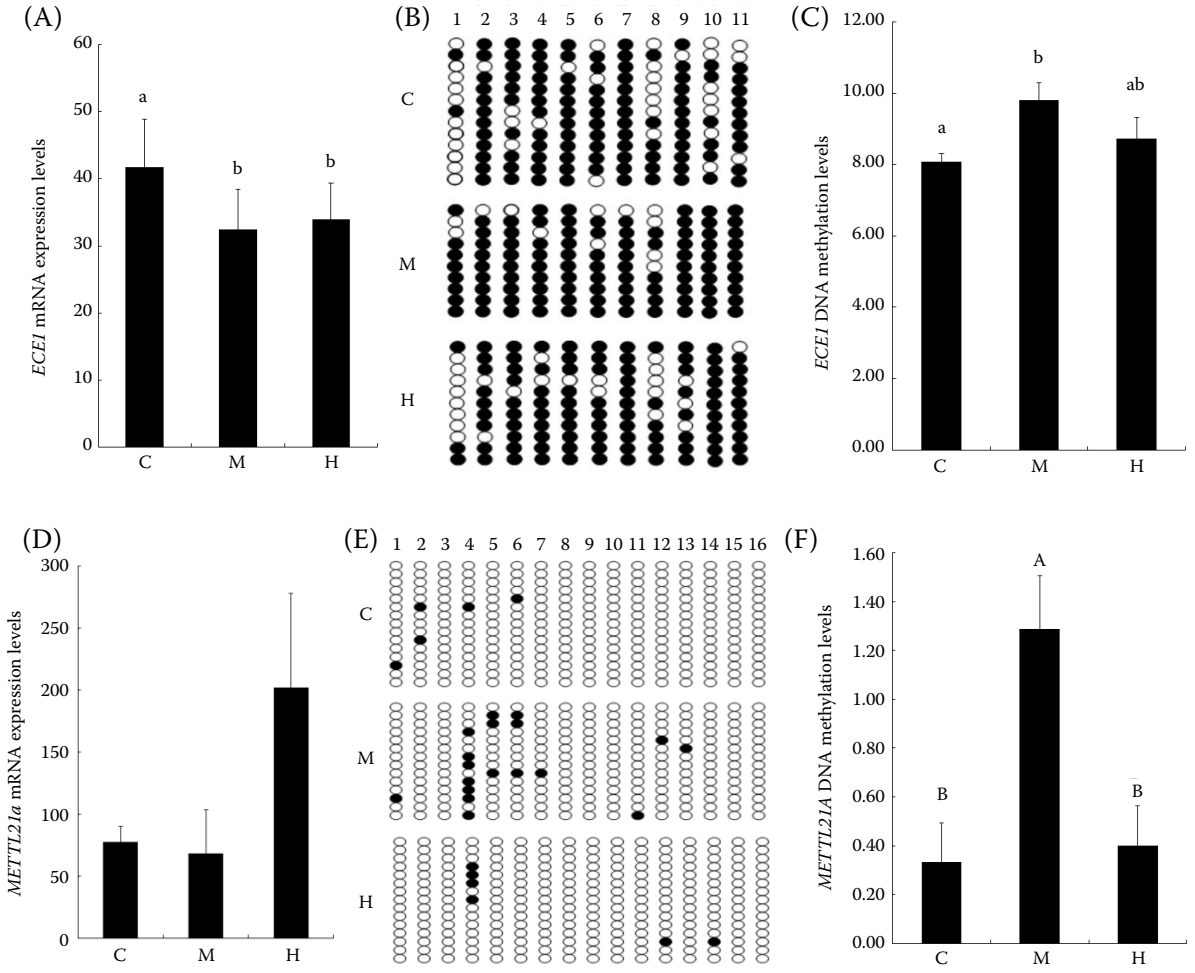

Figure 7. The validation of mRNA expression and methylation of candidate genes

(A) The mRNA expression of *ECE1* among C, M and H groups; (B) The *ECE1* promoter CpG methylation patterns, each horizontal row represents an independent clone and each circle represents a single CpG dinucleotide, and black circles and white circles indicate methylated and unmethylated CpG sites, respectively; (C) The methylation cytosine proportion of *ECE1* promoter CpG region among C, M and H groups; (D) The mRNA expression of *METTL21A* among C, M and H groups; (E) The *METTL21A* promoter CpG methylation patterns; (F) The methylation cytosine proportion of *METTL21A* promoter CpG region among C, M and H groups

[a,b]On the columns mean statistical difference ($P < 0.05$); [A,B]On the columns represent statistical difference ($P < 0.01$)

C = control group (0 mg/kg FA); CpG = cytosine-phosphate-guanine dinucleotide; H = high folic acid group (10 mg/kg FA); M = medium folic acid group (5 mg/kg FA)

https://doi.org/10.17221/102/2025-CJAS

METTL21A were chosen as key candidate genes linking folic acid, DNA methylation, and hepatic lipid metabolism. The mRNA expression levels of *ECE1* in M and H groups were downregulated compared with the C group ($P < 0.05$) (Figure 7A), whereas the proportion of CpG methylation in the promoter of *ECE1* in M group was significantly higher than that of C group ($P < 0.05$) (Figure 7B,C), indicating that the methylation of *ECE1* may inhibit its gene expression. Similarly, the proportion of CpG methylation in the promoter of METTL21A in the M group was significantly higher than that in both the C and H groups ($P < 0.01$) (Figure 7E,F), while no significant difference was observed between the C and H groups ($P > 0.05$) (Figure 7E,F). However, the expression level of METTL21A showed no significant difference among the C, M, and H groups. These results show that the promoter methylation patterns of *ECE1* and *METTL21A* were generally consistent with the RRBS data.

DISCUSSION

The present study investigated whether the dietary folic acid (FA) supplementation modulates hepatic lipid metabolism in broilers through epigenetic reprogramming. Using RRBS for genome-wide DNA methylation profiling, we identified 3 319 differentially methylated regions (DMRs) in the liver in response to FA. These DMRs, evenly distributed between hyper- and hypo-methylated states, were located in both intergenic and promoter regions, suggesting a complex, multi-layered epigenetic response. Subsequent enrichment analyses indicated that the associated genes are involved in critical pathways, particularly fatty acid metabolism, directly linking these epigenetic changes to the hepatic function, the central organ for lipid regulation.

Accumulating evidence has demonstrated that the folic acid (FA) supplementation can modulate DNA methylation patterns across various tissues and species, with implications for metabolic regulation. For instance, a recent study by Kranenburg et al. (2025) showed that FA supplementation (5–10 times above baseline) reduced insulin resistance in high-fat diet-fed mice by altering one-carbon metabolism and DNA methylation patterns of the insulin receptor gene in both hypothalamus and liver (Kranenburg et al. 2025). This highlights the direct link between FA intake, tissue-specific methylation changes, and metabolic outcomes. Similarly, emerging evidence supports the role of FA in the hepatic lipid regulation through epigenetic mechanisms. Song et al. (2025) reported that the paternal FA supplementation in mice alleviated hepatic steatosis in offspring via sperm DNA methylation modifications at key lipid metabolism genes (*Acc1*, *Scd1*). A review by Yang et al. (2025) further consolidates this view, concluding that folate regulates hepatic lipid metabolism in MASLD through one-carbon metabolism and DNA methylation.

Furthermore, Souza et al. (2025) demonstrated that the FA treatment induced differential methylation at 755 CpG sites in human adipocytes, affecting the pathways related to metabolic regulation such as cAMP signalling (Souza et al. 2025). In our previous studies using the same experimental model, we demonstrated that FA supplementation significantly improved growth performance, reduced abdominal fat deposition, and altered hepatic gene expression related to lipid metabolism (Li et al. 2021; Zhang et al. 2021). The present study extends these findings by revealing the epigenetic landscape underlying these phenotypic changes. Notably, the number of DMRs differed between the M and H group compared to the control, suggesting a non-linear dose-response relationship similar to that observed in mammalian models (Kranenburg et al. 2025). Collectively, our integrated analysis, along with recent evidence from mammalian studies, supports the role of FA as a key nutritional modulator of epigenetic regulation in lipid metabolism. Future research should focus on validating the functional consequences of the identified methylation changes.

Among the DMGs, *ECE1* and *METTL21A* were identified as hub genes associated with FA-mediated epigenetic regulation of hepatic lipid metabolism. These genes were selected based on RRBS-detected promoter DMRs, functional relevance to lipid metabolism and methylation, and consistency between methylation and expression. *ECE1* (endothelin converting enzyme 1) is a membrane-bound zinc metalloprotease and a key enzyme in the biosynthesis of endothelin-1 (Lambert et al. 2008). In this study, the FA-induced increase in *ECE1* promoter methylation was associated with a corresponding decrease in its mRNA expression, suggesting an epigenetic silencing effect. This inverse correlation is consistent with the

https://doi.org/10.17221/102/2025-CJAS

canonical repressive role of promoter methylation. Previous research has shown that FA supplementation was unable to rescue defects in *ECE1*-deficient mouse embryos (Haque et al. 2014), further supporting the link between FA and *ECE1* function. *METTL21A* (methyltransferase 21A, HSPA lysine) is a non-histone methyltransferase that specifically modulates the function of Hsp70 proteins and is involved in peptidyl-lysine methylation (Carreras et al. 2020). Interestingly, although 5 mg/kg FA supplementation significantly increased the methylation level of the *METTL21A* promoter, its mRNA expression remained unchanged in the present study. This dissociation may be explained by the specific location of the differentially methylated CpG sites. Not all promoter methylation events are functionally equivalent; methylation at CpG sites distant from transcription start sites or outside transcription factor binding motifs may have a limited impact on transcriptional initiation. Thus, the observed hypermethylation might occur in regions that are not critical for *METTL21A* transcriptional regulation. These findings provide insights into the epigenetic mechanisms by which FA regulates the hepatic lipid metabolism in broilers.

KEGG pathway analysis identified 31 significantly enriched pathways among DMGs in response to FA supplementation, primarily associated with fatty acid metabolism, *TLR* signalling, and the *FoxO* signalling pathway – all critically involved in hepatic lipid regulation. The enrichment of fatty acid metabolism pathways aligns with recent poultry research showing that FA alleviates the fatty liver syndrome by modulating lipid metabolism-related gene expression (Sun et al. 2024). Our results extend these findings by demonstrating that FA alters the methylation of key fatty acid metabolism genes (e.g. *ACADL*, *ECHS1*, *HADH*, *HADHA*), suggesting an epigenetic mechanism underlying FA-mediated lipid regulation. The enrichment of the *TLR* signalling pathway provides another mechanistic link. Liu et al. (2024) demonstrated that one-carbon metabolism, including folate-mediated pathways, orchestrates *TLR4*-driven inflammatory responses. Our observation of methylation changes in *TLR* pathway-related genes suggests that FA may influence hepatic lipid metabolism through immune-metabolic interactions involving *TLR* signalling. Recent evidence further underscores the folate role in hepatic lipid homeostasis. Chi et al. (2024) reported that disturbed folate metabolism impairs autophagic flux and increases hepatocytic lipid accumulation, supporting our observation that FA induces genome-wide methylation changes in pathways central to lipid regulation. The enrichment of the *FoxO* signalling pathway – a key regulator of lipid homeostasis – further supports the multifaceted role of FA in hepatic function. This finding supports the hypothesis that FA regulates hepatic lipid metabolism, at least in part, through the epigenetic modulation of gene expression.

However, several limitations of this study should be acknowledged. The results should be interpreted with caution, as the bisulphite conversion rate assessed using the spike-in lambda DNA control, was <99% (specifically, 98.7%), which could introduce potential false-positive signals. While this limitation may affect the absolute methylation values reported, it is mitigated by our stringent data filtering and the comparative nature of our analysis (control vs treatment), which focuses on differential rather than on absolute methylation. Therefore, the presented absolute methylation levels should be considered preliminary. Future studies with optimised bisulphite conversion, along with validation using independent methods such as bisulphite pyrosequencing, are warranted to confirm these findings.

In conclusion, this study provides the first comprehensive DNA methylome landscape of chicken liver in response to dietary FA supplementation. Our findings reveal that FA alters the methylation of key genes involved in lipid metabolism and epigenetic regulation. Notably, 5 mg/kg FA induced more extensive methylation changes than 10 mg/kg. Based on these epigenetic findings and previously reported phenotypic effects, we recommend 5 mg/kg FA supplementation for broiler production, as it effectively induces beneficial methylation changes, improves growth performance, and reduces fat deposition, while being more economical. These findings support the use of FA as a nutritional strategy to control fat deposition in broiler farming and suggest that identified DMGs could serve as potential epigenetic markers for breeding programmes. Future research should validate the stability and heritability of these methylation changes under field conditions.

Conflict of interest

The authors declare no conflict of interest.

https://doi.org/10.17221/102/2025-CJAS

REFERENCES

Angeloni A, Bogdanovic O. Enhancer DNA methylation: Implications for gene regulation. Essays Biochem. 2019 Dec 20;63(6):707-15.

Carreras J, Hamoudi R, Nakamura N. Artificial intelligence analysis of gene expression data predicted the prognosis of patients with diffuse large B-cell lymphoma. Tokai J Exp Clin Med. 2020 Apr 20;45(1):37-48.

Chi WY, Lee GH, Tang MJ, Chen BH, Lin WL, Fu TF. Disturbed intracellular folate homeostasis impairs autophagic flux and increases hepatocytic lipid accumulation. BMC Biol. 2024 Jul 2;22(1):146.

Du ZQ, Pang YQ, Zhang Y, Wang L, Zhang R, Li H, Yang CX. Folate inhibits lipid deposition via the autophagy pathway in chicken hepatocytes. Poult Sci. 2023 Feb; 102(2):102363.

Friso S, Udali S, De Santis D, Choi SW. One-carbon metabolism and epigenetics. Mol Aspects Med. 2017 Apr;54: 28-36.

Haque A, Sankova B, Kvasilova A, Krejci E, Sedmera D. Does folic acid supplementation rescue defects in ECE-1 -deficient mouse embryos? Folia Biol (Praha). 2014;60(5): 244-51.

Kranenburg E, Kubant R, Cho CE, Yang Z, Datars M, Dong J, Anderson GH. Folic acid reduces insulin resistance in mice with diet-induced obesity by altering one-carbon metabolism and DNA methylation patterns of hypothalamic and hepatic insulin receptor gene. Mol Nutr Food Res. 2025 Oct;69(20):e70181.

Lambert LA, Whyteside AR, Turner AJ, Usmani BA. Isoforms of endothelin-converting enzyme-1 (ECE-1) have opposing effects on prostate cancer cell invasion. Br J Cancer. 2008 Oct 7;99(7):1114-20.

Li X, Zhang Y, Jing W, Tang W, Xing J, Zhang Y. Effects of folic acid supplementation to basal diets of broilers on growth performance, slaughter performance, IGF2 gene expression and methylation. Czech J Anim Sci. 2021;66(12):504-12.

Li Y, Feng Q, Guo M, Wang Y, Jiang Y, Xing J. Genome-wide survey reveals dynamic effects of folate supplement on DNA methylation and gene expression during C2C12 differentiation. Physiol Genomics. 2018 Mar 1;50(3): 158-68.

Liu Y, Zhi L, Shen J, Li S, Yao J, Yang X. Effect of in ovo folic acid injection on hepatic IGF2 expression and embryo growth of broilers. J Anim Sci Biotechnol. 2016 Jul 22; 7:40.

Liu Y, Yang J, Liu X, Liu R, Wang Y, Huang X, Li Y, Liu R, Yang X. Dietary folic acid addition reduces abdominal fat deposition mediated by alterations in gut microbiota and SCFA production in broilers. Anim Nutr. 2022 Sep 25; 12:54-62.

Liu X, Wang C, Li Y, Wang Y, Sun X, Wang Q, Luo J, Lv W, Yang X, Liu Y. Fecal microbiota transplantation revealed the function of folic acid on reducing abdominal fat deposition in broiler chickens mediated by gut microbiota. Poult Sci. 2024 Mar;103(3):103392.

Ma H, Liu H, Yang YT, Han M, Jiang CM. The effect of folate deficiency and different doses of folic acid supplementation on liver diseases. Br J Nutr. 2025 Jan 14;133(1):37-47.

Mattei AL, Bailly N, Meissner A. DNA methylation: A historical perspective. Trends Genet. 2022 Jul;38(7):676-707.

NRC – National Research Council. Nutrient requirements of poultry. 9th revised ed. Washington (DC): National Academies Press; 1994. 176 p.

Song Y, Zhao L, Fu Z, Zhao G, Sun C, Gu W, Tian Z. Paternal folic acid supplementation alleviated hepatic steatosis in male offspring through sperm DNA methylation modification. Mol Nutr Food Res. 2025 Dec;69(24):e70328.

Souza LL, da Mota JCNL, Carvalho LM, Ribeiro AA, Caponi CA, Pinhel MAS, Costa-Fraga N, Diaz-Lagares A, Izquierdo AG, Nonino CB, Crujeiras AB, Nicoletti CF. Genome-wide impact of folic acid on DNA methylation and gene expression in lupus adipocytes: An in vitro study on obesity. Nutrients. 2025 Mar 20;17(6):1086.

Sun X, Ma J, Wang C, Ren Z, Yang X, Yang X, Liu Y. Functional roles of folic acid in alleviating dexamethasone-induced fatty liver syndrome in laying hens. Anim Res One Health. 2024 Jul;3(1):114-28.

Wen Y, Luo J, Shi C, Wu J. Folic acid promotes autophagy to relieve metabolism-associated fatty liver disease by regulating NRF2. Eur J Histochem. 2025 Sep;69(4):4309.

Yang M, Xiao X, Mei J, Pubu-Ciren, Gong Q. MASLD: Insights on the role of folate in hepatic lipid metabolism. Front Nutr. 2025 Jul 16;12:1583674.

Yu X, Liu R, Zhao G, Zheng M, Chen J, Wen J. Folate supplementation modifies CCAAT/enhancer-binding protein α methylation to mediate differentiation of preadipocytes in chickens. Poult Sci. 2014 Oct;93(10): 2596-603.

Zhang Y, Zhang N, Liu L, Wang Y, Xing J, Li X. Transcriptome analysis of effects of folic acid supplement on gene expression in liver of broiler chickens. Front Vet Sci. 2021 Sep 16;8:686609.

Received: July 14, 2025
Accepted: June 17, 2026
Published online: July 24, 2026